© 2018. Published by The Company of Biologists Ltd | Journal of Cell Science (2018) 131, jcs219824. doi:10.1242/jcs.219824

RESEARCH ARTICLE

Hepatocyte-like cells reveal novel role of SERPINA1 in transthyretin amyloidosis

Christoph Niemietz, Lutz Fleischhauer*, Vanessa Sandfort, Sarah Guttmann, Andree Zibert and Hartmut H.-J. Schmidt‡

ABSTRACT

Transthyretin (TTR)-related familial amyloid polyneuropathy (ATTR) results from aggregation and extracellular disposition of misfolded TTR mutants. Growing evidence suggests the importance of hepatic chaperones for the modulation of pathogenesis. We took advantage of induced pluripotent stem cell (iPSC)-derived hepatocyte-like cells (HLCs) from ATTR patients (ATTR-HLCs) to compare chaperone gene expression to that in HLCs from healthy individuals (H-HLCs). From the set of genes analyzed, chaperones that are predominantly located extracellularly were differently expressed. Expression of the chaperones showed a high correlation with *TTR* in both ATTR-HLCs and H-HLCs. In contrast, after *TTR* knockdown, the correlation was mainly affected in ATTR-HLCs suggesting that differences in TTR expression triggers aberrant chaperone expression. Serpin family A member 1 (SERPINA1) was the only extracellular chaperone that was markedly upregulated after *TTR* knockdown in ATTR-HLCs. Co-immunoprecipitation revealed that SERPINA1 physically interacts with TTR. *In vitro* assays indicated that SERPINA1 can interfere with TTR aggregation. Taken together, our results suggest that extracellular chaperones play a crucial role in ATTR pathogenesis, in particular SERPINA1, which may affect amyloid formation.

KEY WORDS: SERPINA1, Transthyretin, Chaperones, Disease modeling, Induced pluripotent stem cells (iPSCs)

INTRODUCTION

Transthyretin amyloidosis (ATTR) is a rare, progressive disease caused by mutations of transthyretin (TTR). ATTR is thought to result from the formation of amyloid fibrils, primarily affecting the peripheral autonomic nervous system and the heart (Conceição et al., 2016). More than 100 disease-causing mutations of the *TTR* gene have been described. TTR displays extensive β-sheet structures prone to self-oligomerization (Blake and Serpell, 1996). TTR is a tetrameric protein and it is assumed that kinetic instability of mutant proteins favors fibril formation (Foss et al., 2005). TTR synthesis and secretion into the blood predominantly takes place in the liver, while minor sites of synthesis (<5%) include the choroid plexus, retinal pigment epithelium, pancreas, placenta and the Schwann cells (Buxbaum et al., 2014; Cavallaro et al., 1990; Schreiber, 2002). TTR functions as a plasma protein responsible for the transport of thyroxine (T4) and the retinol-binding protein (RBP4), which acts as a carrier for retinol (vitamin A) (Monaco et al., 1995; Neumann et al., 2001). $TTR^{-/-}$ mice, however, do not show significant signs of disease and are fertile (Wei et al., 1995).

The impact of the protein quality control (PQC) system has been associated to the pathogenesis of amyloidotic diseases, e.g. in amyotrophic lateral sclerosis (ALS), Alzheimer's and Parkinson's disease (Daturpalli et al., 2013; Park et al., 2018; Wang et al., 2014). Several lines of evidence suggest that PQC, operative during the synthesis of TTR in the hepatocyte, is also an important determinant of ATTR. In a pioneering work, biophysical and secretion assays suggested the contribution of endoplasmic reticulum (ER)-assisted folding by cell type-specific chaperones (Sekijima et al., 2005). TTR mutations ATTRD18G and ATTRA25T, both associated with late-onset ATTR of the central nervous system, are found at low concentrations in the blood (Hammarström et al., 2003; Sekijima et al., 2003). For ATTRD18G, low secretion efficiency has been observed in HEK cells, suggesting that ER retention of misfolded TTR results in the induction of the unfolded protein response (UPR), including upregulation of the ER chaperone glucose-regulated protein 78 (GRP78) (Sato et al., 2007). More recently, proteome analysis (2D-DIGE) following expression of the TTR mutation ATTRL55P in yeast revealed the induction of chaperones that mediate protein folding, including members of the HSP70, peptidyl-prolyl-cis-trans isomerase (PPIase) and ubiquitin-like modifier (SUMO) families (Gomes et al., 2012). Several TTR mutations were shown to be subjected to ER-associated degradation (ERAD) pathways (Sato et al., 2012). Multi-dimensional protein identification technology (MudPIT) profiling of adipose tissue has suggested the overexpression of several chaperones in ATTR patients (Brambilla et al., 2013). Of note, proteome analyses of plasma from ATTRV30M patients indicated altered expression of several extracellular chaperones (da Costa et al., 2015).

The protease inhibitor SERPINA is also highly expressed in the liver and strongly secreted into blood (Topic et al., 2012). *SERPINA1* deficiency results in a genetic disorder resulting in damage of the liver and the lung due to uncontrolled neutrophil elastase and non-functional SERPINA1 in the liver (Radlovic et al., 2014). Direct interaction of TTR and SERPINA1, however, has not yet been described.

Whereas previous studies analyzed whole liver, human serum, adipose tissue or a variety of standard cell culture lines, such as HEK293 cells, to assess the impact of PQC on gene expression, we took advantage of hepatocyte-like cells (HLCs) differentiated from induced pluripotent stem cells (iPSCs). Gene expression of chaperones related to amyloidosis was explored by real-time qPCR analysis in HLCs with the intrinsic genetic background of ATTR patients, i.e. in HLCs derived from ATTR patients (ATTR-HLCs). TTR knockdown in HLCs was employed to study the relation of TTR and individual chaperone gene expression. We

Medizinische Klinik B für Gastroenterologie und Hepatologie, Universitätsklinikum Münster, 48149 Münster, Germany.
*Present address: Fakultät für angewandte Naturwissenschaften und Mechatronik, Hochschule München, 80335 München, Germany.

‡Author for correspondence (hepar@ukmuenster.de)

C.N., 0000-0002-9393-8748; S.G., 0000-0001-8419-9501; A.Z., 0000-0002-5188-450X; H.H.-J.S., 0000-0002-2402-7764

Received 9 May 2018; Accepted 18 September 2018

Journal of Cell Science (2018) 131, jcs219824. doi:10.1242/jcs.219824

identified SERPINA1 as a highly regulated chaperone in ATTR-HLCs. Further analyses revealed a physical interaction of SERPINA1 with TTR as well as its interference with TTR aggregation, suggesting that SERPINA1 represents a novel target for therapy of ATTR.

RESULTS

Comparison of cells derived from ATTR patients and healthy donors

In this study, ATTR-HLCs were used to assess chaperone gene expression. HLCs from healthy individuals (H-HLCs) served as control. The characteristics of the four ATTR cell lines and the four cell lines derived from healthy individuals are given in Table S1. We used a protocol for reprogramming and differentiation that has been shown to be very robust in terms of variability (Niemietz et al., 2016). After reprogramming of primary patient cells, the cells displayed typical iPS cell colony growth (Fig. 1A), high immunofluorescence staining of pluripotent stem cell markers OCT4, NANOG, SSEA-4, and TRA-1-60 (Fig. 1B), high mRNA levels of embryonic stem cell-specific markers *OCT4*, *NANOG* and *SOX2* (Fig. 1C), and expected expression levels in the trilineage hPSC Scorecard™ Assay (Fig. 1D) suggesting that typical iPSCs have been derived from ATTR patients and healthy individuals. After a 14 day differentiation protocol of iPSCs, the cells showed their characteristic polygonal shape and high nuclear to cytoplasmic ratio that is typical of HLCs (Fig. 1E), overall high immunofluorescence staining of albumin, HNF4A and TTR (Fig. 1F), high glycogen storage (Fig. 1G), and high expression levels of the hepatocyte marker genes serum albumin (*ALB*), apolipoprotein A1 (*APOA1*), ATPase copper transporting Beta (*ATP7B*), nuclear constitutive androstane receptor (*NR1I3*, also known as CAR) and transferrin (*TF*) (Fig. 1H). These data indicate that phenotypes, function as well as expression levels of hepatocyte marker genes are almost identical in iPSCs and HLCs derived from ATTR patients and healthy controls, when cells were subjected to the reprogramming and differentiation protocols. Importantly, variation was low between expression of hepatic marker genes in HLCs derived from H-HLCs and ATTR-HLCs when using at least two clones per line (±s.e.<1.1) (Fig. S1).

Almost identical TTR expression in HLCs derived from ATTR patients and healthy individuals

Since the relation of TTR to chaperone gene expression was of high importance to our study, we further assessed whether overall TTR expression might differ between ATTR-HLCs and H-HLCs. *TTR* mRNA and TTR protein secreted into the cell culture medium by HLCs did not differ between both groups (Fig. 2A,B). Of note, *TTR* mRNA levels observed in HLCs were similar to those in primary human hepatocytes, suggesting that HLCs model human hepatocytes (Niemietz et al., 2016). We also inspected the different forms of TTR by western blot analyses and did not observe differences between both groups of HLCs (Fig. 2C), suggesting that any deviation that might be observed for chaperone gene expression between ATTR-HLCs and H-HLCs was not biased by the level of TTR expression.

Gene expression of extracellular chaperones is predominantly affected in HLCs derived from ATTR patients

Having verified that TTR appears to be synthesized and secreted in a similar manner and magnitude in both groups of HLCs, RT-qPCR analyses of chaperone genes were performed. In total, 39 genes were investigated (Table S2). Selection of genes was based on PubMed searches for genes reported to be associated with protein folding, degradation, ubiquitylation and translational arrest in amyloidotic dieseases, such as ATTR, amyotrophic lateral sclerosis (ALS), Alzheimer's disease, amyloid light-chain (AL) amyloidosis and amyloid A (AA) amyloidosis. All genes were first validated in human hepatoma HepG2 cells and found to be robustly expressed (data not shown). The expression of the chaperone genes was categorized according to a threshold of fold-change (FC) that takes into account the variability of hepatocyte marker expression (FC<±2.5). A FC≥±5 (two times that of the mean hepatic marker gene variability) was chosen to indicate significance of chaperone gene expression between groups. Of note, differences in individual chaperone gene expression in the cell lines were low (±s.e.<1.3) (Fig. S2). Five chaperone genes, i.e. *SERPINA1*, fibrinogen alpha chain (*FGA*), fibrinogen beta chain (*FGB*), alpha-2-macroglobulin (*A2M*) and heat shock protein beta-1 (*HSPB1*), were found to differ in at least two ATTR-HLC lines, whereas 34 genes showed expression levels below the threshold (Fig. 3). Expression levels of *SERPINA1* and *FGA* differed in three ATTR-HLC lines. Upregulation was found for *FGA* (3 ATTR-HLC lines), *A2M* (2 ATTR-HLC lines) and *FGB* (2 ATTR-HLC lines). Downregulation was observed for *HSPB1* (2 ATTR-HLC lines). *SERPINA1* displayed upregulation in one ATTR-HLC line and downregulation in two ATTR-HLC lines. However, variation in *SERPINA1* expression was very low in the four H-HLC lines suggesting that variability due to different donors to generate HLCs is generally low (Fig. S3). Of note, four of the genes (*SERPINA1*, *FGA*, *A2M* and *FGB*) belong to a group of seven chaperones that are predominantly located extracellularly (da Costa et al., 2015). In contrast, 32 chaperones that have been reported to predominantly show intracellular localization did not exceed a FC≥±5, indicating different expression levels in ATTR-HLCs as compared to H-HLCs (Fig. 3).

SERPINA1 expression is closely related to that of TTR in HLCs

Chaperone gene expression in HLCs could be associated to the overall level of TTR expression. We used small interfering RNAs (siRNA) and antisense oligonucleotides (ASO) for knockdown of TTR expression in the HLCs (Niemietz et al., 2016). As expected, TTR downregulation was almost identical in ATTR-HLCs and H-HLCs resulting in an mRNA knockdown of 75% to 85% and a protein knockdown of 67% to 85% (Fig. S4). The expression of the five chaperones (SERPINA1, FGA, A2M, FGB and HSPB1) that were found to be differently regulated in at least two ATTR-HLC lines (Fig. 3) were examined for the effect of TTR knockdown. First, the correlation coefficient of *TTR* mRNA before and after knockdown was determined in H-HLCs and ATTR-HLCs (Fig. 4A,B). Whereas no correlation (r<0.1) was observed for *HSPB1*, a high correlation (r>0.7) was observed for the other chaperone genes prior TTR knockdown in H-HLCs and ATTR-HLCs. However, after TTR knockdown, the correlation coefficient significantly (r>0.5) dropped in ATTR-HLCs. Inspection of the chaperone mRNA level after TTR knockdown revealed a significant increase of *SERPINA1* in ATTR-HLCs, whereas no induction was observed for H-HLCs (Fig. 4C), and the other chaperone genes were only marginally affected by TTR knockdown in both HLC groups. Patient-specific analysis of *TTR* mRNA expression in the four ATTR-HLC lines indicated an upregulation of *SERPINA1* mRNA in three out of four patient-specific HLC lines (Fig. 4D). Secretion of SERPINA1 from HLCs after TTR knockdown was also assessed. No significant change in SERPINA1 levels was observed after TTR knockdown for H-HLCs, whereas SERPINA1 protein levels were

Journal of Cell Science (2018) 131, jcs219824. doi:10.1242/jcs.219824

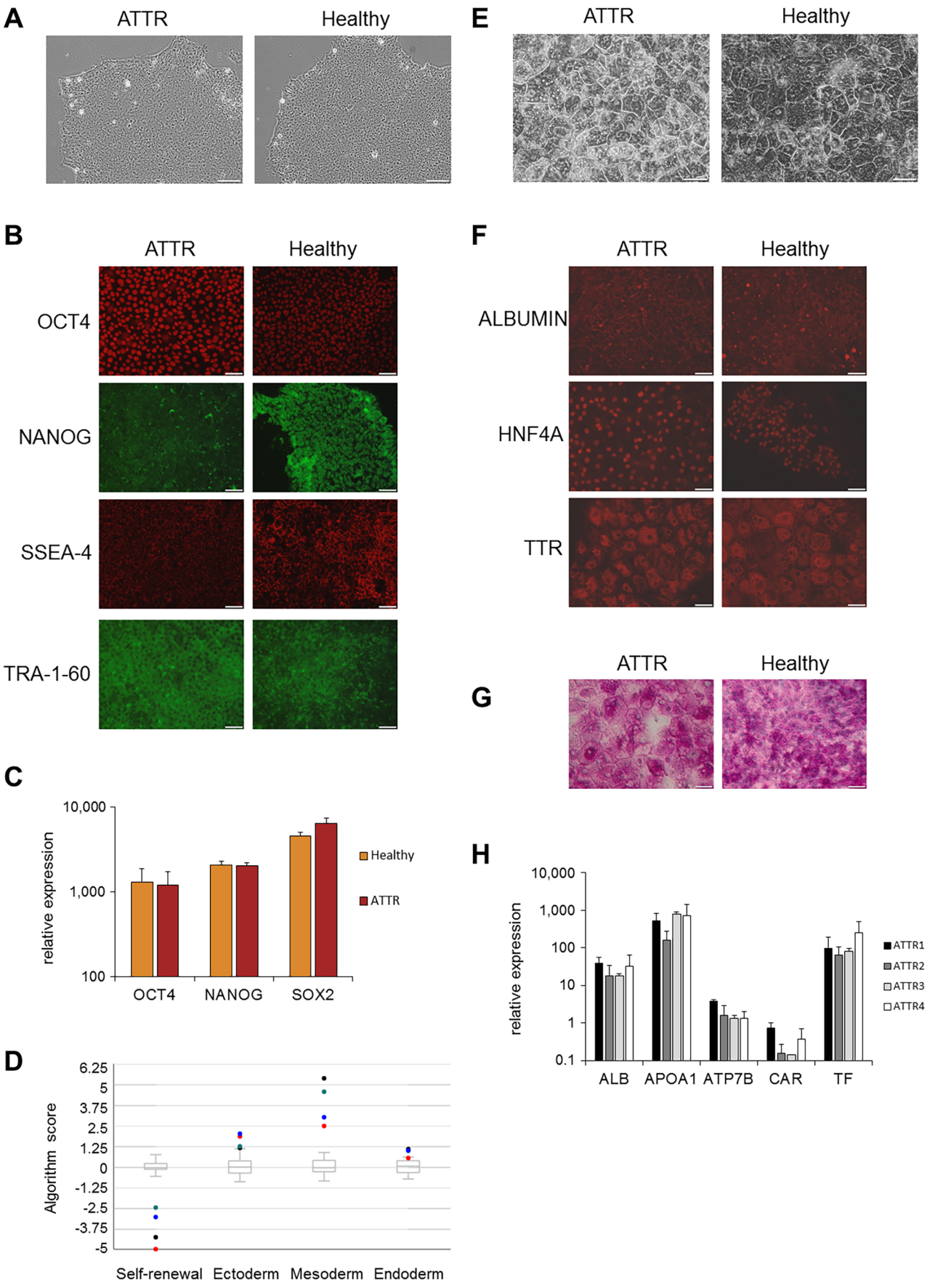

Fig. 1. See next page for legend.

Journal of Cell Science (2018) 131, jcs219824. doi:10.1242/jcs.219824

Fig. 1. Similar molecular and phenotypical characteristics of cells obtained from ATTR patients and healthy individuals. (A) Brightfield images of cell colonies derived from ATTR and healthy individuals after reprogramming. Scale bars: 100 µm. (B) Immunofluorescence after reprogramming. Scale bars: 50 µm. (C) mRNA expression of markers indicating pluripotency. Values derived from four ATTR-HLCs and four H-HLCs are shown (data from three different experimental repeats). (D) Sample scores of EBs relative to an undifferentiated reference set. ATTR (red, green) and donor-EBs established from healthy individuals (black, blue) are representatively shown. (E) Brightfield images showing hepatic differentiation of iPSC-derived cells at day 14. Scale bars: 50 µm. (F) Immunofluorescence stains of iPSC-derived cells at day 14 of hepatic differentiation. Scale bars: 50 µm. (G) PAS reaction indicating glycogen synthesis of cells at day 14 of hepatic differentiation. One typical experiment is shown. Scale bars: 50 µm. (H) RT-qPCR results of five liver markers expressed in four ATTR-HLCs at day 14 of hepatic differentiation (data from three different experimental repeats).

elevated in three of four ATTR-HLCs (Fig. 4E), suggesting that – in ATTR-HLCs – SERPINA1 represents a chaperone that is inversely correlated to expression of TTR.

SERPINA1 physically interacts with TTR

High levels of SERPINA1 and TTR are found in human serum. However, a physical interaction between SERPINA1 and TTR has not been reported. We assessed interaction of SERPINA1 and TTR by co-immunoprecipitation using cell culture supernatants derived from HLCs. First, expression of SERPINA1 was determined by western blot analysis of HLC cell culture supernatants. A single protein band of ∼55 kDa was observed in the supernatants of ATTR-HLCs and H-HLCs, which is similar to that in human plasma samples (Fig. 5A). Next, HLC cell culture supernatants were incubated with anti-TTR antibody for pull-down using immunobeads, followed by western blot analysis to detect co-precipitated SERPINA1. A SERPINA1-specific band was observed for cell culture supernatants derived from ATTR-HLCs and H-HLCs (Fig. 5B). Of note, SERPINA1 could not be precipitated from HLC supernatants when non-specific antibody was used for pull-down. Densitometric quantification of the SERPINA1 co-immunoprecipitates relative to the loading control

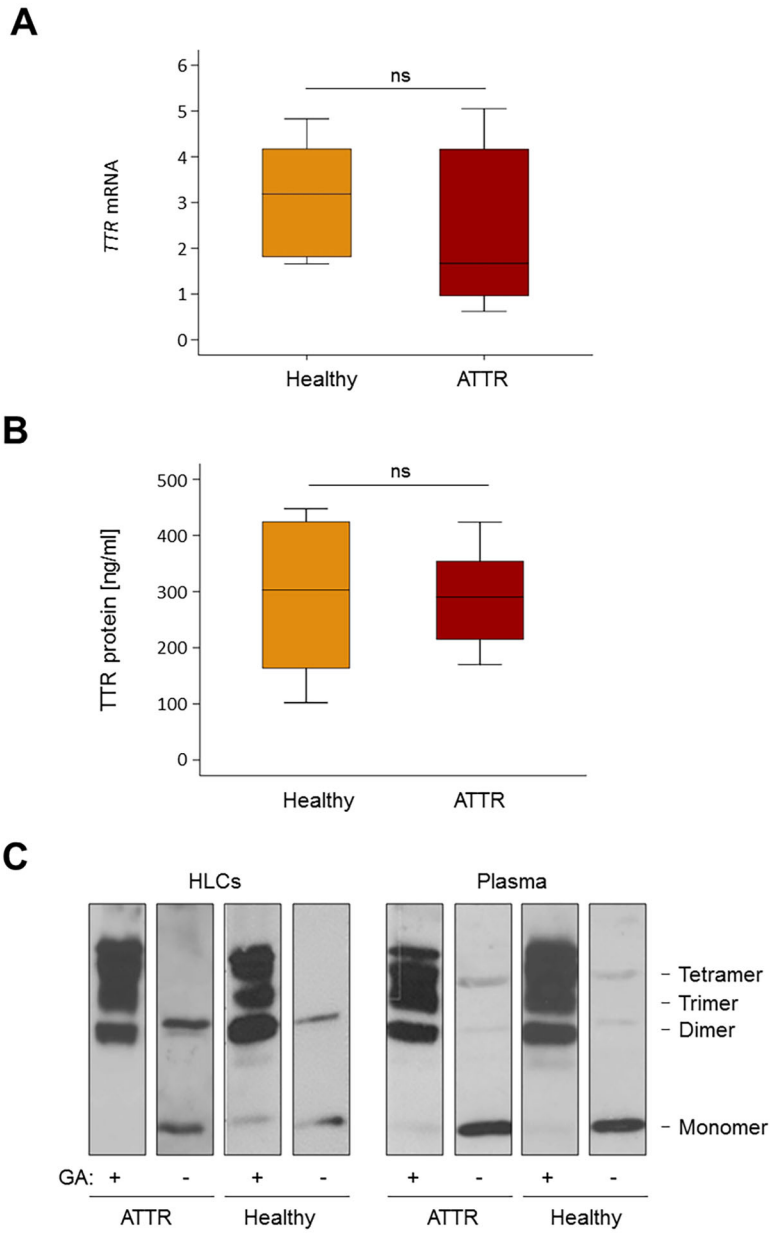

Fig. 2. Similar TTR expression in HLCs derived from ATTR patients and healthy individuals. (A) Boxplot representation of *TTR* mRNA expression in four ATTR-HLCs and four H-HLCs. ΔCt versus *GAPDH* was determined (data from three different experimental repeats). (B) Boxplot representation of TTR protein determined in the supernatants of four ATTR-HLCs and four H-HLCs by ELISA (data from three different experimental repeats). (C) Western blot analysis of TTR expression in HLCs; 15 µl of cell culture supernatant derived from ATTR-HLCs and H-HLCs was subjected to SDS-PAGE. Glutaraldehyde (GA) of supernatants is indicated. Blots were derived from different gels and assembled according to molecular weight standards. Plasma (1 µl) served as a control. One of three typical experiments is shown.

Journal of Cell Science (2018) 131, jcs219824. doi:10.1242/jcs.219824

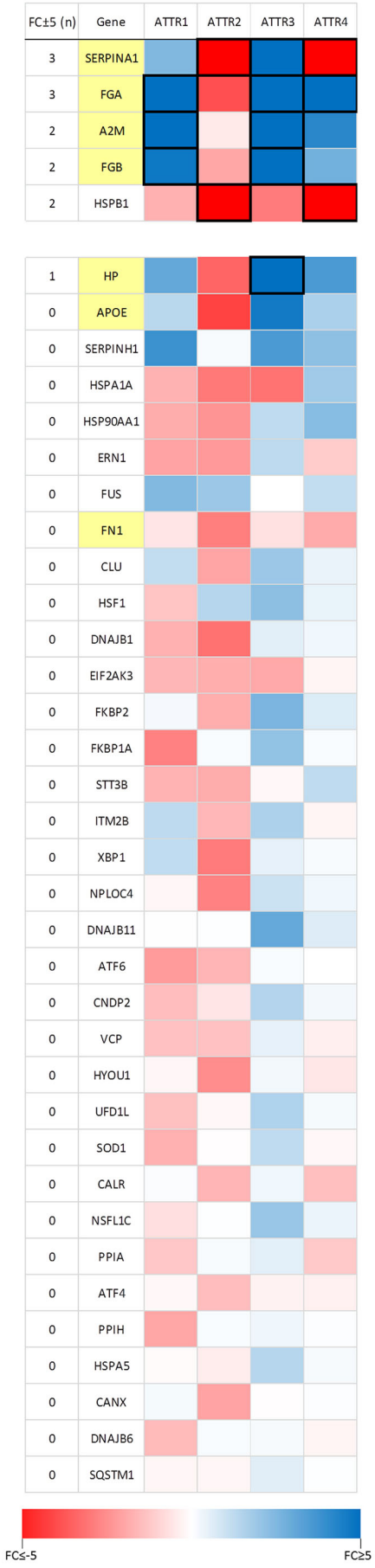

Fig. 3. Extracellular expression of chaperone genes was dominantly affected in ATTR-HLCs as compared to H-HLCs. mRNA expression of 39 chaperone genes in ATTR-HLCs was compared relative to mean expression levels of H-HLCs. The fold-change (FC) was determined and is represented in a heat map. Numbers of ATTR-HLC lines that show expression levels above the threshold (FC±5) are indicated. Chaperones predominantly located extracellularly are highlighted (yellow). Data from three different experimental repeats are shown.

revealed that 37.4±8.6% of SERPINA1 was pulled-down, suggesting that significant amounts of SERPINA1 physically interact with TTR. However, no differences in the amount of precipitated SERPINA1 was observed when cell culture supernatants of ATTR-HLCs and H-HLCs were used, suggesting that both wild-type and mutant TTR are bound to SERPINA1. To assess the interaction of SERPINA1 and TTR using an alternative method, a hybrid ELISA was employed (Fig. 5C). Positive values of absorbance relative to controls were observed when cell culture supernatants of ATTR-HLCs were used (OD_{450} ≈1.6). Moreover, analysis of human plasma also resulted in above-background TTR detection values. Omission of anti-SERPINA1 antibody or the use of mouse sera containing human TTR and murine SERPINA1 did not produce above-background values (data not shown), indicating the specificity of the assay.

SERPINA1 attenuates formation of high molecular forms of TTR

We further explored the nature of interaction between SERPINA1 and TTR by addressing TTR aggregation – an intrinsic event of ATTR. To establish an *in vitro* TTR aggregation assay, a previously described method employing the acidic denaturation of wild-type TTR (Klabunde et al., 2000) was used with modifications. After acidic denaturation of human TTR, the soluble and insoluble fractions, i.e. supernatant and pellet, were assessed by centrifugation followed by western blotting of TTR. After 72 h at pH 4.6, high molecular forms (HMFs) of TTR were significantly increased in the insoluble fraction (Fig. 6A,B). In contrast, such forms were not observed without incubation at 37°C (0 h) or at neutral pH, suggesting that treatment at low pH for several hours is a prerequisite for the formation of TTR HMFs. To further assess the specificity of the assay, we asked whether Tafamidis, a known stabilizer of TTR that inhibits TTR fibril formation (Chen et al., 2016), interferes with TTR aggregation. Pre-incubation with Tafamidis significantly reduced formation of TTR HMFs in a dose-dependent manner (Fig. S5), suggesting that the *in vitro* assay is suitable to detect interference of TTR aggregation. While pre-incubation with recombinant SERPINA1 did not fully inhibit the formation of HMFs present in the insoluble fraction, almost the same amount of HMFs was repeatedly observed in the soluble fraction (Fig. 6C,D). In contrast, recombinant albumin used as control did not interfere with formation of TTR HMFs, suggesting that SERPINA1 specifically hampers the conversion of soluble TTR into insoluble HMFs. Densitometric quantification revealed that addition of SERPINA1 significantly increased the relative amount of HMFs by ∼2-fold in the soluble fraction as compared to untreated control (0.86±0.06 and 0.37±0.04, respectively) (Fig. 6C,D).

DISCUSSION

In this study, we analyzed the gene expression of genes that have been previously associated with chaperone function, to assess the role of the PQC system for aberrant TTR expression in the hepatocyte. An iPSC-based cell model was used to determine the expression levels in hepatic cells. Of note, in contrast to liver-derived patient cells, the cells studied here were not subjected to

Journal of Cell Science (2018) 131, jcs219824. doi:10.1242/jcs.219824

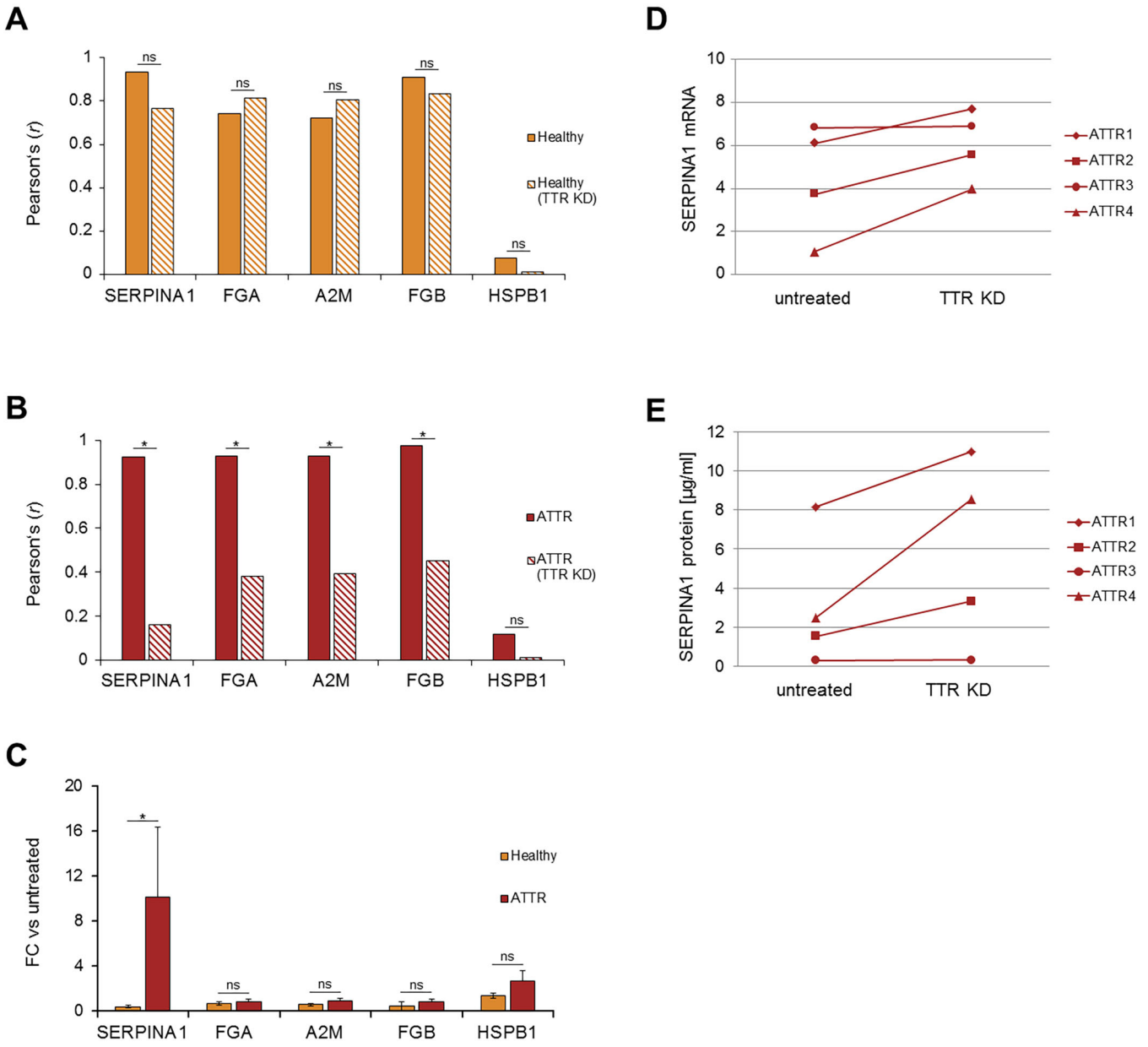

Fig. 4. SERPINA1 is closely related to TTR expression in HLCs. (A,B) Correlation of TTR with chaperone genes in H-HLCs (A) and ATTR-HLCs (B). Correlation factor (r) was calculated before and after TTR knockdown (data from four different experimental repeats). (C) mRNA expression of chaperone genes after TTR knockdown. Data were set relative to untreated controls (data from four different experimental repeats). (D,E) SERPINA1 mRNA expression (D) and protein levels (E) before and after TTR knockdown in the four ATTR-HLC lines (data from three different experimental repeats). *P<±0.05; ns, not significant.

secondary regulation by other organs or factors present in the blood. In our cohort of chaperone genes chosen for qRT-PCR analysis of HLCs, we observed that expression of several genes was significantly different in ATTR-HLCs as compared to H-HLCs. Notably, chaperones predominantly associated to extracellular location were affected in ATTR-HLCs, whereas genes primarily involved in ERAD and UPR pathways were mostly expressed at levels found in cells that had been derived from healthy individuals. Both last-mentioned systems have been described to fail detection of TTR mutants – i.e. ATTR-L55P and ATTR-V122I – that show high thermodynamic stability resulting in high secretion efficiency (Chen et al., 2014; Sekijima et al., 2005). Accordingly, ATTRV30M, which we investigated here in two ATTR-HLC lines, had been classified to have similar thermodynamic stability as wild-type TTR (Sato et al., 2007; Sekijima et al., 2005). In addition, ATTRG47A and ATTRR34T, the other two amyloidogenic mutations studied, share central clinical parameters with ATTRV30M (González-Duarte et al., 2013; Patrosso et al., 1998). Our observation, therefore, indicates that transcription mediated through ERAD and UPR pathways is not significantly affected in the presence of TTR mutants with a high thermodynamic stability.

Microarray analyses of liver biopsy samples, the current gold standard to assess differently regulated hepatic gene expression in ATTR, indicated a modulation of ER-associated proteins in patients carrying ATTRV30M (Norgren et al., 2014), e.g. gene expression of FK506 binding protein 2 (FKBP2) was significantly downregulated. In our study, a disparate regulation of this gene was not observed. However, apart from the different processing events of cells and RNA

Journal of Cell Science (2018) 131, jcs219824. doi:10.1242/jcs.219824

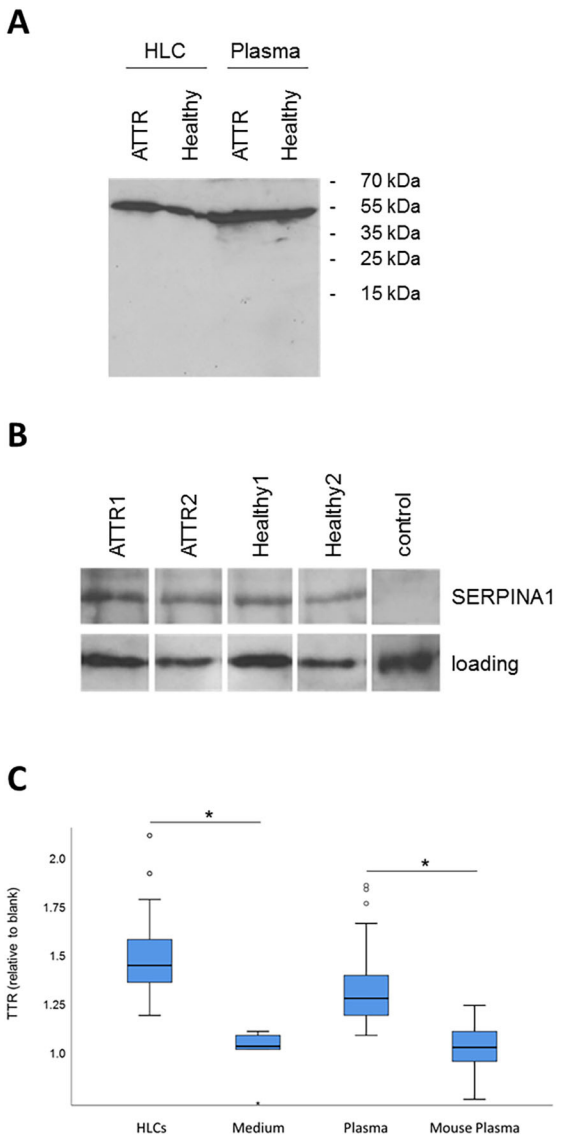

Fig. 5. SERPINA1 is bound by TTR in cell culture supernatants of HLCs. (A) Western blot analysis of SERPINA1 expressed by HLCs. Cell culture supernatant (15 µl) derived from ATTR-HLCs or H-HLCs was subjected to SDS-PAGE. Plasma (1 µl per lane) is shown as a control. (B) Co-immunoprecipitation of TTR and SERPINA1. Cell culture supernatants derived from ATTR-HLCs and H-HLCs were subjected to immunoprecipitation using anti-TTR antibody followed by western blotting of SERPINA1. Loading control (15 µl) before immunoprecipitation is shown. As control, unrelated antibody was used for pull-down. One of three typical experiments is shown. (C) Hybrid ELISA using capture antibody against SERPINA1 and detection antibody against TTR. OD values were set relative to control (blank) at 1.0. Box plot representation of four ATTR-HLC cell culture supernatants (diluted 1:10) and three ATTR plasma samples (diluted 1:5000). Non-conditioned cell culture medium and murine sera were used as controls (data from five different experimental repeats). **P*<0.05.

that were used used to determine gene expression in the two approaches, other factors, such as age of patients, influence of blood-borne growth factors and course of disease may affect levels of gene expression. HLCs derived from iPSC have been previously used for gene expression studies, also involving a few chaperone genes (Leung et al., 2013). The gene encoding heat shock protein family A (Hsp70) member 1A (*HSPA1A*) was one chaperone that was found to be slightly overexpressed (~2-fold). We found *HSPA1A* to be differently expressed in two ATTR-HLCs (FC<−2.7). We might have missed the biological significance of this and other minor mRNA dysregulations of chaperone genes as we have chosen a high internal threshold (FC<±5) to indicate significance.

In our study, *SERPINA1*, *FGA*, *A2M*, *FGB* and *HSPB1* were found to be highly expressed in ATTR-HLCs as compared to H-HLCs. Of these, HSPB1 is the only chaperone that is predominantly found intracellularly. Gene expression was found to be downregulated in two ATTR-HLCs, while two other patient-specific cell lines that displayed minor downregulation did not exceed a threshold of FC±5 (Fig. 3). HSPB1 is known to induce sequestration of beta-amyloid and is induced in the brains of mice transgenic for the human amyloid precursor protein (Ojha et al., 2011). Thus, HSPB1 may be overrepresented in neuronal cells exposed to amyloid fibrils (Santos et al., 2008) but may have similar functions in hepatocytes, although TTR amyloid deposition is not observed in the liver.

Of the chaperones identified in this study, fibrinogen is the only chaperone that has previously been reported to directly interact with TTR (da Costa et al., 2011; Tang et al., 2009b). The chaperone activity of FGA is based on the isoform fibrinogen-420 (Tang et al., 2009a), and glycation of FGA results in a loss of function (Fonseca et al., 2016). Moreover, FGA can cause amyloid deposition as a consequence of genetic mutation (Yazaki et al., 2018). Also, cross-seeding by FGA has to be considered as one possible mechanism by which amyloidic proteins spread, mostly worsening disease (Sakai et al., 2017; Verma et al., 2018). However, aggregation-prone proteins have also been shown to inhibit crosslinking of amyloidogenic proteins. Interestingly, this role has been described for monomeric TTR, which has been shown to interfere with beta-amyloid oligomerization (Garai et al., 2018; Li et al., 2013). It must, however, be taken into account that beneficial and disease-promoting elements can be closely related.

A2M has been identified to inhibit amyloid fibril formation of aggregation-prone proteins in other diseases, such as Alzheimer's disease (Yerbury et al., 2009). Of note, *FGA*, *FGB* and *A2M* encode for acute-phase proteins, i.e. proteins whose plasma concentration increase or decrease in response to inflammation (Jain et al., 2011), suggesting that upregulation of these genes is a characteristic of ATTR (Suenaga et al., 2017). At least two patient-specific ATTR-HLC cell lines exhibited upregulation of *FGA*, *FGB* and *A2M*. In line, previous studies also report an induction of the three chaperones in plasma samples of ATTRV30M patients (da Costa et al., 2015), corroborating the validity of our HLC model. Overexpression of these chaperones in our cell model, therefore, indicates that such regulation is due to the intrinsic synthesis of mutant TTR in the hepatocyte, rather than to a secondary regulative response. It can be assumed that *FGA*, *FGB* and *A2M* work synergistically, enabling hepatocytes to cope with amyloidogenic TTR. Although expression of *FGA* and *FGB* is correlated to result in functional fibrinogen, we can only speculate on the role of A2M to contribute to a complex cluster of chaperones targeting protein aggregates (Wyatt et al., 2012; Yerbury et al., 2009; Zsila, 2010). Although in our approach several chaperones were identified to be associated with ATTR pathogenesis, a rather small and heterogeneous patient group, encompassing three different mutations and early/late onset of disease, was studied. While our data suggest that chaperone expression differs in hepatic cells of ATTR patients and of healthy individuals, a genotype- and phenotype-specific analysis needs a higher number of patients.

SERPINA1 was identified as a chaperone in amyloidoses, and is part of amyloid aggregates in Alzheimer's disease and ALS (Howlett and Moore, 2006; Zsila, 2010). In ATTR, SERPINA1 was found to be upregulated in plasma of ATTR patients (da Costa et al.,

Journal of Cell Science (2018) 131, jcs219824. doi:10.1242/jcs.219824

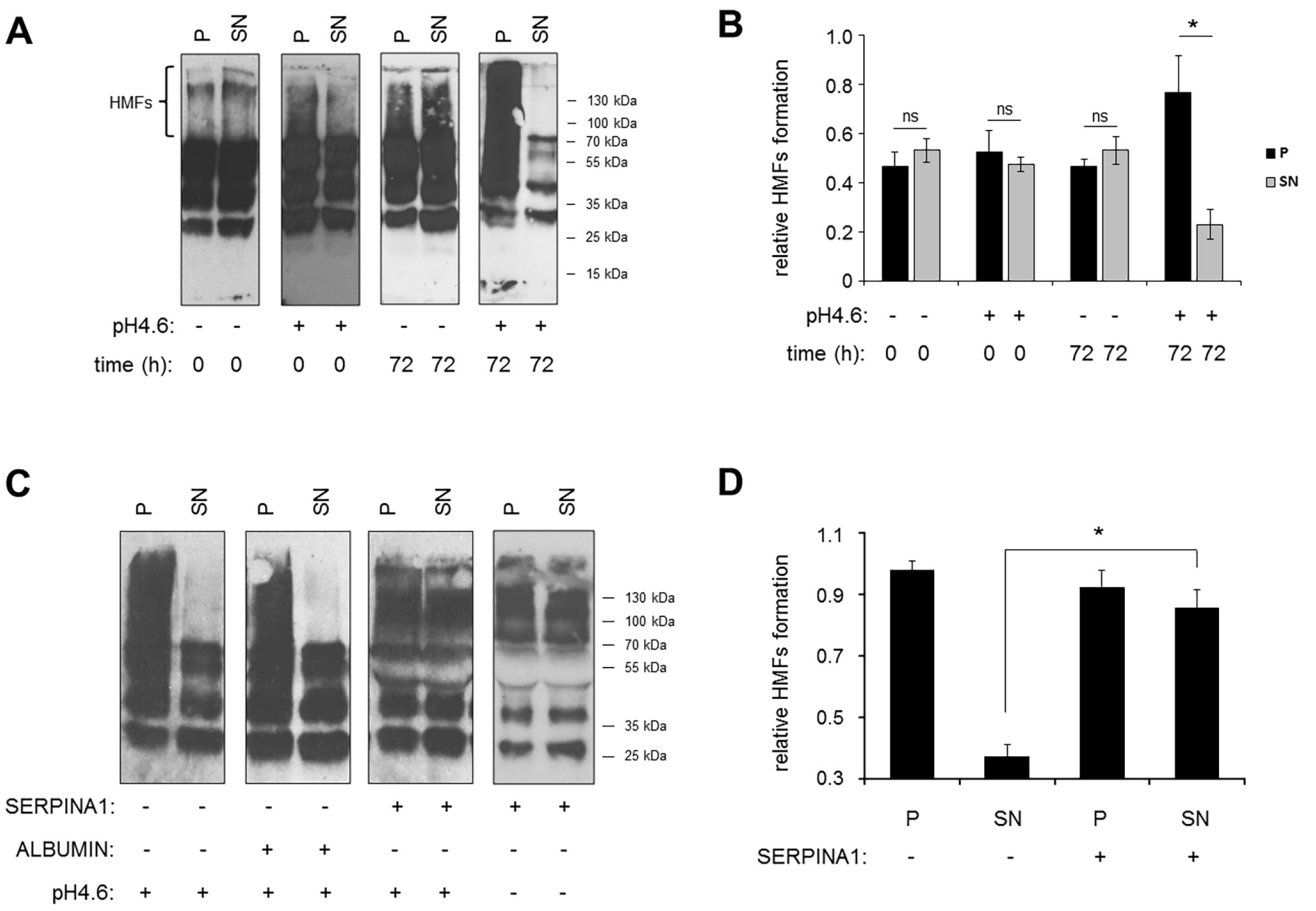

Fig. 6. SERPINA1 attenuates formation of high molecular forms of TTR. (A) TTR protein (1 µg) was exposed to HMF formation by using acetate buffer (pH 4.6) and incubated for indicated time points. After centrifugation and glutaraldehyde treatment, pellet (P) and supernatant (SN) fractions were subjected to SDS-PAGE followed by western blot analysis of TTR. (B) Relative amounts of P and SN fractions were determined by densitometric quantification (data from three different experimental repeats). (C) Formation of high molecular form (HMF) TTR was determined in the presence of SERPINA1 and albumin at 60 ng/ml. Treatment of TTR at pH 7.4 is shown as control. (D) Densitometric quantification of relative HMF formation in P and SN fractions was determined in presence and absence of SERPINA1 (data from three different experimental repeats). *P<0.05; ns, not significant.

2015). Our findings indicate upregulation of *SERPINA1* mRNA in one ATTR-specific hepatic cell line and downregulation in two other cell lines, while one cell line did not show disparate expression levels as compared to healthy individuals. To our knowledge decreased levels of SERPINA1 have not been reported for ATTR; however, Alzheimer's patients show low SERPINA1 liquor levels (Hansson et al., 2009). As our ATTR patient cohort was low, the course of SERPINA1 regulation in hepatocytes cannot be proposed. However, *SERPINA1* represents one of the most-regulated genes in our cohort of hepatic cell0073, suggesting that it is highly responsive to aberrant TTR expression in hepatocytes.

The important role of SERPINA1 in ATTR is emphasized again in our study by analysis of *TTR* knockdown. SERPINA1 expression was inversely correlated with TTR levels after knockdown, suggesting a mutual dependence of both genes. Intriguingly, investigations of serum TTR and SERPINA1 levels in cells of patients suffering various diseases indicates opposed levels of expression (Bag et al., 2014; Fatima et al., 2017; Raju M. et al., 2016). Although the exact molecular regulation of opposite expression levels remains to be unraveled, IL-6 driven induction of gene expression following inflammation might play a role. It is, therefore, tempting to speculate that the process of inflammation in ATTR modulates disease (Gonçalves et al., 2017). Furthermore, our data indicate for the first time that TTR directly interacts with SERPINA1. Although we did not detect any difference in the binding of SERPINA1 to wild-type or mutant TTR in our immunoprecipitation assay, subtle differences might exist *in vivo*, depending on the TTR mutant expressed by ATTR patients.

A protocol involving acid-mediated TTR aggregation was used in our study and resulted in high-molecular forms (HMFs) of TTR as observed after western blot analysis. Since the detection of HMFs depended on glutaraldehyde treatment prior to SDS gel electrophoresis, we assume that HMFs are highly labile. Staining of HMFs with Congo Red failed, possibly due to interference with glutaraldehyde (data not shown). Our data indicate that SERPINA1 interferes with TTR aggregation, suggesting that the chaperone can hamper a conversion of the soluble form into insoluble aggregates. Aggregation into self-assembled fibrils of SERPINA1 has been reported together with concurrent inhibition of these oligomers by SERPINA1 fragments (Janciauskiene et al., 1995). Several proteins, including serum amyloid P-component (SAP), apolipoprotein, complement binding factors and clusterin, have been found in amyloid deposits of patients (Azevedo et al., 2011; Klein et al., 2011), suggesting that interaction of TTR with serum proteins is common. Although binding of serum proteins to TTR may take place at different steps of amyloid formation and has diverse functional consequences, it has previously been proposed that clusterin preferentially binds to TTR monomers, resulting in the

blocking of the first molecular events (Greene et al., 2015). However, as shown in our study, clusterin was not differently regulated in HLCs of ATTR patients. In the presence of the TTR tetramer stabilizer Tafamidis, we observed a specific pattern of HMFs that differed from the HMF pattern after addition of SERPINA1. Thus, we hypothesize that SERPINA1 binds to both wild-type TTR and mutant TTR, and reduces fibril formation during a phase other than that of TTR tetramer stabilization. By contrast, low levels of SERPINA1 might be unfavorable, as suggested by studies on ATTR patients with SERPINA1 deficiency. An early onset of disease after liver transplantation was reported (Guttmann et al., 2017).

The PQC system might represent an alternative therapy approach to target amyloidosis. Promising studies, e.g. for Alzheimer's disease, focus on proteins of the BRICHOS family (Cohen et al., 2015; Willander et al., 2012b). It has previously been suggested that domains proSP-C and Bri2 can delay fibrillation of Aß40 and Aß42 (Willander et al., 2012b). Proteins of the heat shock family have been demonstrated to efficiently regulate fibril length of α-synuclein, e.g. in Parkinson's disease (Gao et al., 2015; Nillegoda et al., 2015). For ATTR, it has been shown in cell culture that induction of *ATF6* results in reduced secretion of aggregation-prone TTR, possibly impeding pathogenic fibril deposition (Chen et al., 2014; Shoulders et al., 2013). Although our work here adds several chaperones – most importantly SERPINA1 – to the growing search for other therapy strategies to treat ATTR, we were unable to decipher the exact biological mechanisms the identified chaperones use for pathogenesis.

In order to determine chaperone gene expression, we used iPSC-derived cell lines. As noted earlier, iPSC-based approaches can have shortcomings due to incomplete reprogramming and differentiation, most prominently when comparing different donors (Kajiwara et al., 2012; Ortmann and Vallier, 2017). Although we addressed variability by using identical protocols for iPSC generation and hepatic differentiation and an overall low variability of marker gene expression – including *TTR* and *SERPINA1* – was observed, a bias due to the heterogeneity of cell population cannot be excluded. Within the limitations of our approach, our data suggest that SERPINA1 has a role in ATTR pathogenesis, possibly by inhibiting the formation of large TTR aggregates. Our data also indicate that a concerted modulation of – mostly extracellular – chaperone genes is induced in ATTR patients; this might be part of a complex proteostasis network, resulting in an adaptive response to aberrant TTR expression (van Oosten-Hawle and Morimoto, 2014).

MATERIALS AND METHODS

Ethics statement

All samples were obtained in accordance with ethics committee of the Universitätsklinikum Münster. Participants were informed regarding the use of data and informed consent was obtained in writing from all individuals enclosed in the study.

Isolation of urine-derived cells

12-well cell culture plates (Greiner Bio-One, Kremsmünster, Austria) were coated with 0.1% gelatin (Merck Millipore, Darmstadt, Germany). Briefly, urine was centrifuged at 400 ***g*** for 10 min and cell pellets were washed with 50 ml of cold PBS (Sigma-Aldrich, St. Louis, MO), 1% penicillin–streptomycin (Pen–Strep; Thermo Fisher Scientific, Waltham, MA). After a second centrifugation, cell pellets were resuspended in UC medium [DMEM/F-12 (Life Technologies, Carlsbad, CA) supplemented with 10% FCS (Thermo Fisher Scientific), 1% Pen–Strep, 1×MEM non-essential amino acid solution (NEAA, Sigma-Aldrich), 1× GlutaMAX-I (Life Technologies), 0.1 mM 2-mercaptoethanol (Life Technologies) and SingleQuot Kit CC-4127 REGM (Lonza, Basel, Switzerland)]. Cells were resuspended in 1 ml of UC medium and incubated at 37°C with 5% CO_2 for 24 h. Half of the medium was changed daily. At confluence, cells were expanded for two passages (p2). Typically – and independently from the initial urine volume – 4×10^6 cells were obtained after 3 weeks of cell culture.

Generation of iPSCs

Approximately 0.5×10^6 of urine-derived cells at p2 were transfected with 1 µg of pCXLE-hOCT3/4-shp53-F, pCXLE-hSK and pCXLE-hUL (Addgene plasmids #27077, #27078 and #27080, respectively) by using the Amaxa Basic Nucleofector Kit for Primary Mammalian Epithelial Cells (VPI-1005, Lonza, Basel, Switzerland). Subsequently, cells were transferred to Matrigel® matrix (Corning, Corning, NY) coated 6-well cell culture plates (Greiner Bio-One) and cultured for 24 h in UC medium. At day 1, UC medium was replaced with serum-free complete cell culture medium mTeSR-1 (Stemcell Technologies, Vancouver, BC, Canada) supplemented with 1% Pen–Strep. iPSC colonies were subcultured every 7 days by using 1 U/ml Dispase (Stemcell Technologies).

Hepatic differentiation

iPSC lines showing stable growth characteristics were transferred into single-cell suspensions using Accutase solution (Sigma-Aldrich). Typically, one 6-well cell culture plate with $4–5\times10^6$ cells was used for hepatic differentiation. After 24 h, culture medium was replaced for 3 days with DMEM/F12, 100 ng/ml recombinant activin-A (PeproTech Germany, Hamburg, Germany), 100 ng/ml fibroblast growth factor-2 (FGF2, PeproTech Germany) and 50 ng/ml recombinant human Wnt3a (R&D Systems, Minneapolis, MN) using increasing concentrations of KnockOut SR Xenofree CTS (KSR, Life Technologies) of 0.2–2.0%. The next 8 days, cells were cultured in DMEM/F12 supplemented with 10% KSR, 1 mM NEAA, 1 mM L-glutamine, 1% dimethyl sulfoxide (Sigma-Aldrich) and 100 ng/ml hepatocyte growth factor (HGF, Peprotech). To induce hepatic maturation, cells were treated for the final 3 days with DMEM/F12 supplemented with 10% KSR, 1 mmol/l NEAA, 1 mM L-glutamine and 0.1 µM dexamethasone (Sigma-Aldrich).

Immunocytochemistry

Following fixation with 4% paraformaldehyde (Electron Microscopy Sciences) and permeabilization with 0.5% Triton X-100 (Thermo Fisher Scientific), cells grown in a 12-well plate ($1–2\times10^6$ cells) were blocked with 3% bovine serum albumin solution (BSA, Sigma-Aldrich) and stored at 4°C until staining. Primary and secondary antibodies were diluted in 1% BSA solution. Anti-albumin antibody (ab2406, Abcam, Cambridge, UK), anti-TTR antibody (A0002, Dako, Glostrup, Denmark), anti-HNF4a antibody (sc-6556, Santa Cruz Biotechnology, Dallas, TX) and anti-NANOG antibody (sc-33759, Santa Cruz Biotechnology) were used at 1:100. Anti-Oct4 antibody (60093PE, Stemcell Technologies), anti-SSEA-4 antibody (60062PE, Stemcell Technologies) and anti-TRA-1-60 antibody (60064AD, Stemcell Technologies) were used at 1:200. Antibodies against Alexa Fluor 488 (A11001, Invitrogen, Carlsbad, CA), Alexa Fluor 568 (A11057, Invitrogen) and Alexa Fluor 594 (A11012, Invitrogen) were used at 1:500. Samples were incubated with primary antibody for 2 h, and with secondary antibody for 1 h at 4°C. Photographs were taken using an Olympus CKX41-X10 microscope with cellSens Standard 1.11 imaging software.

Quantitative real-time PCR

Cell pellets derived from one 6-well cell culture plate were used to isolate whole RNA using the RNeasy Mini Kit (Qiagen, Hilden, Germany) and 1 µg of RNA was applied for first-strand synthesis using the SuperScript™ III First-Strand Synthesis SuperMix for qRT-PCR kit (Invitrogen). Of the reverse transcriptase product 1 µl was mixed with Takyon ROX SYBR Master Mix Blue dTTP (Eurogentec, Lüttich, Belgium) and 150 nM of primers (Table S2). qPCR was analyzed on the ABI Prism 7900 HT Sequence Detection System (Applied Biosystems, Foster City, CA). Data were analyzed by SDS 2.4 software (Applied Biosystems). Ct values were normalized to *GAPDH* and evaluated using the comparative Ct method ($2^{-\Delta\Delta Ct}$).

hPSC scorecard assay

Embryoid bodies were established as previously described (Niemietz et al., 2016). 1×10^6 cells were used to generate embryoid bodies. Briefly, iPSC clusters were cultured for 7 days in 6-well suspension culture plates (Greiner Bio-One) according to the manufacturer's protocol (TaqMan® hPSC Scorecard™). The trilineage differentiation potential was examined using the 384-well hPSC Scorecard™ Panel (Life Technologies) followed by evaluation using the Thermo Fisher Cloud hPSC Scorecard Analysis software.

Periodic acid-Schiff reaction

Glycogen synthesis of HLCs was assessed at day 14 of hepatic differentiation by periodic acid-Schiff (PAS) reaction using the system protocol (395B-1KT, Sigma-Aldrich).

TTR knockdown

HLCs at day 14 of hepatic differentiation were transferred to Opti-MEM (Gibco). siTTR1 (Alnylam Pharmaceuticals, Cambridge, MA) was added at 0.3 µM to the medium. TTR-ASO (IONIS Pharmaceuticals, Carlsbad, CA) was mixed at 1.5 µM with 2.5 µl Lipofectamine 2000 Reagent (Life Technologies). Scrambled oligonucleotides were used as control. Cell culture supernatants were harvested daily for 3 days.

SDS-PAGE and western blotting

Lysates derived from a 6-well plate were prepared using RIPA buffer (60 mM tris-HCl, 150 mM NaCl, 2% Na-deoxycholate, 2% Triton X-10, 0.2% SDS and 15 mM EDTA) in the presence of protease inhibitors (Roche, Complete Mini, EDTA-free) and separated on 10–12.5% SDS polyacrylamide gels. For blotting Amersham Protran Premium 0.45 nitrocellulose (GE Healthcare Life Sciences, Buckinghamshire, UK) was used. After overnight blocking in 5% non-fat dry milk (AppliChem, Darmstadt, Germany) blots were incubated in Tris-buffered saline (TBS)/0.05% Tween 20 (Sigma-Aldrich). Anti-TTR antibody (A0002, Dako) and anti-SERPINA1 antibody (843285, R&D Systems) were used at 1:1000 in 0.05% TBS-T with 0.5% non-fat milk for 1 h. Anti-goat HRP (ab97110, Abcam) and anti-rabbit HRP (ab6721, Abcam) were used at 1:10,000. Amersham ECL Western Blotting Detection Reagent (GE Healthcare Life Sciences) was applied. All blots were quantified by using ImageJ 1.50i analysis software.

ELISA

ELISA of human TTR and SERPINA1

ELISA of TTR was performed as reported elsewhere (Coelho et al., 2013). Briefly, Nunc 96-well MaxiSorp™ plates (44240421, Thermo Fisher Scientific) were coated overnight with anti-TTR antibody (A0002, Dako) in 50 mM carbonate/bicarbonate buffer (C3041-50CAP, Sigma-Aldrich) at 4°C. After washing, samples were diluted in 1× powerblock (HK085-5K, Biogenex, Fremont). Cell culture supernatants were used at 1:10 and human plasma samples were used at 1:19,600. For standard curve calculation, TTR (P1742-5MG, Sigma-Aldrich) was applied. Detection was by ab9015 (Abcam; at 1:2500) and alkaline-phosphate conjugation by A5187-1ML (Sigma-Aldrich). Colorimetric detection was performed by p-Nitrophenyl phosphate addition (N2770-50SET, Sigma-Aldrich). Absorbance was determined at 405 nm. Human SERPINA1 DuoSet ELISA (DY1268, R&D Systems) was used according to the manufacturer's instruction. Cell culture supernatants were used at 1:4000 and in 5% Tween 20 in PBS. TMB substrate (555214, BD Biosciences, Franklin Lakes, NJ) was used for colorimetric detection. Absorbance was determined at 450 nm. Hybrid ELISA was performed with goat anti-human SERPINA1 antibody (843285, R&D Systems) for capture and with sheep anti-human TTR antibody (ab9015, Abcam) for detection.

In vitro TTR aggregation

Human TTR (P1742, Sigma-Aldrich) was reconstituted in 1× powerblock (BioGenex, Fremont, CA) and incubated under acidic conditions to induce TTR aggregation. 1 µg of TTR was mixed with 1× volume of 200 mM acetate buffer containing 100 mM KCl and 1 mM EDTA (pH 4.6). Samples were incubated at 37°C for 72 h prior centrifugation at 20,000 ***g***, 4°C for 30 min. The supernatant was carefully removed from the pellet and both fractions were treated with 2.5% glutaraldehyde solution (340855, Sigma-Aldrich). Samples were subjected to TTR western blotting thereafter.

Co-immunoprecipitation

Cell culture supernatant (15 µl) derived from 6-well plates was precleared with A/G Plus-Agarose beads (sc2003, Santa Cruz Biotechnology). Beads were mixed with 2 µg of anti-TTR antibody (A0002, Dako) and incubated with precleared samples in non-denaturing RIPA buffer (20 mM Tris HCl pH 8, 137 mM NaCl, 1% Triton X-100, 2 mM EDTA) and protease inhibitors while shaking at 4°C for 24 h. The next day, samples were washed 5× with PBS, centrifuged at 1000 ***g*** for 30 s and subjected to 12.5% PAGE.

Statistical analyses

Statistical analyses were performed by using Kruskal–Wallis one-way ANOVA and Student's *t*-test using SPSS 25 software. Data are given as mean±standard error (±s.e.m.). Correlation of two genes was determined by using Pearson's equation followed by Fisher's *z*-transformation.

Acknowledgements

We are grateful to O. Nadzemova for excellent technical assistance.

Competing interests

The authors declare no competing or financial interests.

Author contributions

Conceptualization: C.N., V.S., A.Z., H.H.-J.S.; Methodology: C.N., L.F., A.Z.; Validation: C.N., A.Z.; Formal analysis: C.N., L.F., A.Z.; Investigation: C.N., L.F., V.S., S.G.; Data curation: A.Z.; Writing - original draft: C.N., A.Z., H.H.-J.S.; Writing - review & editing: V.S., S.G., A.Z., H.H.-J.S.; Visualization: C.N., A.Z.; Supervision: V.S., A.Z., H.H.-J.S.; Project administration: A.Z., H.H.-J.S.

Funding

This research received no specific grant from any funding agency in the public, commercial or not-for-profit sectors.

Supplementary information

Supplementary information available online at
http://jcs.biologists.org/lookup/doi/10.1242/jcs.219824.supplemental

References

Azevedo, E. P. C., Pereira, H. M., Garratt, R. C., Kelly, J. W., Foguel, D. and Palhano, F. L. (2011). Dissecting the structure, thermodynamic stability, and aggregation properties of the A25T transthyretin (A25T-TTR) variant involved in leptomeningeal amyloidosis: identifying protein partners that co-aggregate during A25T-TTR fibrillogenesis in cerebrospinal fluid. *Biochemistry* **50**, 11070-11083.

Bag, A. K., Saha, S., Sundar, S., Saha, B., Chakrabarti, A. and Mandal, C. (2014). Comparative proteomics and glycoproteomics of plasma proteins in Indian visceral leishmaniasis. *Proteome Sci.* **12**, 48.

Blake, C. and Serpell, L. (1996). Synchrotron X-ray studies suggest that the core of the transthyretin amyloid fibril is a continuous β-sheet helix. *Structure* **4**, 989-998.

Brambilla, F., Lavatelli, F., Di Silvestre, D., Valentini, V., Palladini, G., Merlini, G. and Mauri, P. (2013). Shotgun protein profile of human adipose tissue and its changes in relation to systemic amyloidoses. *J. Proteome Res.* **12**, 5642-5655.

Buxbaum, J. N., Roberts, A. J., Adame, A. and Masliah, E. (2014). Silencing of murine transthyretin and retinol binding protein genes has distinct and shared behavioral and neuropathologic effects. *Neuroscience* **275**, 352-364.

Cavallaro, T., Martone, R. L., Dwork, A. J., Schon, E. A. and Herbert, J. (1990). The retinal pigment epithelium is the unique site of transthyretin synthesis in the rat eye. *Invest. Ophthalmol. Vis. Sci.* **31**, 497-501.

Chen, J. J., Genereux, J. C., Qu, S., Hulleman, J. D., Shoulders, M. D. and Wiseman, R. L. (2014). ATF6 activation reduces the secretion and extracellular aggregation of destabilized variants of an amyloidogenic protein. *Chem. Biol.* **21**, 1564-1574.

Chen, J. J., Genereux, J. C., Suh, E. H., Vartabedian, V. F., Rius, B., Qu, S., Dendle, M. T. A., Kelly, J. W. and Wiseman, R. L. (2016). Endoplasmic reticulum proteostasis influences the oligomeric state of an amyloidogenic protein secreted from mammalian cells. *Cell Chem. Biol.* **23**, 1282-1293.

Coelho, T., Adams, D., Silva, A., Lozeron, P., Hawkins, P. N., Mant, T., Perez, J., Chiesa, J., Warrington, S., Tranter, E. et al. (2013). Safety and efficacy of RNAi therapy for transthyretin amyloidosis. *N Engl. J. Med.* **369**, 819-829.

Cohen, S. I. A., Arosio, P., Presto, J., Kurudenkandy, F. R., Biverstål, H., Dolfe, L., Dunning, C., Yang, X., Frohm, B., Vendruscolo, M. et al. (2015). A molecular

chaperone breaks the catalytic cycle that generates toxic Abeta oligomers. *Nat. Struct. Mol. Biol.* **22**, 207-213.
Conceição, I., González-Duarte, A., Obici, L., Schmidt, H. H.-J., Simoneau, D., Ong, M.-L. and Amass, L. (2016). "Red-flag" symptom clusters in transthyretin familial amyloid polyneuropathy. *J. Peripheral Nervous Syst.* **21**, 5-9.
da Costa, G., Gomes, R. A., Guerreiro, A., Mateus, É., Monteiro, E., Barroso, E., Coelho, A. V., Freire, A. P. and Cordeiro, C. (2011). Beyond genetic factors in familial amyloidotic polyneuropathy: protein glycation and the loss of fibrinogen's chaperone activity. *PLoS ONE* **6**, e24850.
da Costa, G., Ribeiro-Silva, C., Ribeiro, R., Gilberto, S., Gomes, R. A., Ferreira, A. N., Mateus, É., Barroso, E., Coelho, A. V., Freire, A. P. et al. (2015). Transthyretin amyloidosis: chaperone concentration changes and increased proteolysis in the pathway to disease. *PLoS ONE* **10**, 1-17.
Daturpalli, S., Waudby, C. A., Meehan, S. and Jackson, S. E. (2013). Hsp90 inhibits alpha-synuclein aggregation by interacting with soluble oligomers. *J. Mol. Biol.* **425**, 4614-4628.
Fatima, I., Sadaf, S., Musharraf, S. G., Hashmi, N. and Akhtar, M. W. (2017). CD5 molecule-like and transthyretin as putative biomarkers of chronic myeloid leukemia - an insight from the proteomic analysis of human plasma. *Sci. Rep.* **7**, 40943.
Fonseca, D., Gilberto, S., Ribeiro-Silva, C., Ribeiro, R., Guinote, I. B., Saraiva, S., Gomes, R. A., Mateus, E., Viana, A., Barroso, E. et al. (2016). The role of fibrinogen glycation in ATTR: evidence for chaperone activity loss in disease. *Biochem. J.* **473**, 2225-2237.
Foss, T. R., Wiseman, R. L. and Kelly, J. W. (2005). The pathway by which the tetrameric protein transthyretin dissociates. *Biochemistry* **44**, 15525-15533.
Gao, X., Carroni, M., Nussbaum-Krammer, C., Mogk, A., Nillegoda, N. B., Szlachcic, A., Guilbride, D. L., Saibil, H. R., Mayer, M. P. and Bukau, B. (2015). Human Hsp70 disaggregase reverses Parkinson's-linked alpha-synuclein amyloid fibrils. *Mol. Cell* **59**, 781-793.
Garai, K., Posey, A. E., Li, X., Buxbaum, J. N. and Pappu, R. V. (2018). Inhibition of amyloid beta fibril formation by monomeric human transthyretin. *Protein Sci.* **27**, 1252-1261.
Gomes, R. A., Franco, C., Da Costa, G. A., Planchon, S. B., Renaut, J., Ribeiro, R. M., Pinto, F., Silva, M. S., Coelho, A. V., Freire, A. P. et al. (2012). The proteome response to amyloid protein expression in vivo. *PLoS ONE* **7**, e50123.
Gonçalves, N. P., Moreira, J., Martins, D., Vieira, P., Obici, L., Merlini, G., Saraiva, M. and Saraiva, M. J. (2017). Differential expression of Cathepsin E in transthyretin amyloidosis: from neuropathology to the immune system. *J. Neuroinflammation* **14**, 115.
González-Duarte, A., Lem-Carrillo, M. and Cárdenas-Soto, K. (2013). Description of transthyretin S50A, S52P and G47A mutations in familial amyloidosis polyneuropathy. *Amyloid* **20**, 221-225.
Greene, M. J., Klimtchuk, E. S., Seldin, D. C., Berk, J. L. and Connors, L. H. (2015). Cooperative stabilization of transthyretin by clusterin and diflunisal. *Biochemistry* **54**, 268-278.
Guttmann, S., Röcken, C., Schmidt, M., Grünewald, I., Zibert, A., Stypmann, J., Schilling, M. and Schmidt, H. (2017). De novo hereditary (familial) amyloid polyneuropathy (FAP) in a FAP liver recipient. *Amyloid* **24**, 126-127.
Hammarström, P., Sekijima, Y., White, J. T., Wiseman, R. L., Lim, A., Costello, C. E., Altland, K., Garzuly, F., Budka, H. and Kelly, J. W. (2003). D18G transthyretin is monomeric, aggregation prone, and not detectable in plasma and cerebrospinal fluid: a prescription for central nervous system amyloidosis? *Biochemistry* **42**, 6656-6663.
Hansson, S. F., Andréasson, U., Wall, M., Skoog, I., Andreasen, N., Wallin, A., Zetterberg, H. and Blennow, K. (2009). Reduced levels of amyloid-beta-binding proteins in cerebrospinal fluid from Alzheimer's disease patients. *J. Alzheimer's Dis.* **16**, 389-397.
Howlett, G. J. and Moore, K. J. (2006). Untangling the role of amyloid in atherosclerosis. *Curr. Opin. Lipidol.* **17**, 541-547.
Jain, S., Gautam, V. and Naseem, S. (2011). Acute-phase proteins: as diagnostic tool. *J. Pharmacy Bioallied Sci.* **3**, 118-127.
Janciauskiene, S., Carlemalm, E. and Eriksson, S. (1995). In vitro fibril formation from alpha 1-antitrypsin-derived C-terminal peptides. *Biol. Chem. Hoppe-Seyler* **376**, 415-424.
Kajiwara, M., Aoi, T., Okita, K., Takahashi, R., Inoue, H., Takayama, N., Endo, H., Eto, K., Toguchida, J., Uemoto, S. et al. (2012). Donor-dependent variations in hepatic differentiation from human-induced pluripotent stem cells. *Proc. Natl. Acad. Sci. USA* **109**, 12538-12543.
Klabunde, T., Petrassi, H. M., Oza, V. B., Raman, P., Kelly, J. W. and Sacchettini, J. C. (2000). Rational design of potent human transthyretin amyloid disease inhibitors. *Nat. Struct. Biol.* **7**, 312-321.
Klein, C. J., Vrana, J. A., Theis, J. D., Dyck, P. J., Dyck, P. J., Spinner, R. J., Mauermann, M. L., Bergen, H. R., III, Zeldenrust, S. R. and Dogan, A. (2011). Mass spectrometric-based proteomic analysis of amyloid neuropathy type in nerve tissue. *Arch. Neurol.* **68**, 195-199.
Leung, A., Nah, S. K., Reid, W., Ebata, A., Koch, C. M., Monti, S., Genereux, J. C., Wiseman, R. L., Wolozin, B., Connors, L. H. et al. (2013). Induced pluripotent stem cell modeling of multisystemic, hereditary transthyretin amyloidosis. *Stem Cell Rep.* **1**, 451-463.
Li, X., Zhang, X., Ladiwala, A. R. A., Du, D., Yadav, J. K., Tessier, P. M., Wright, P. E., Kelly, J. W. and Buxbaum, J. N. (2013). Mechanisms of transthyretin inhibition of beta-amyloid aggregation in vitro. *J. Neurosci.* **33**, 19423-19433.
Monaco, H. L., Rizzi, M. and Coda, A. (1995). Structure of a complex of two plasma proteins: transthyretin and retinol-binding protein. *Science* **268**, 1039-1041.
Neumann, P., Cody, V. and Wojtczak, A. (2001). Structural basis of negative cooperativity in transthyretin. *Acta Biochim. Pol.* **48**, 867-875.
Niemietz, C. J., Sauer, V., Stella, J., Fleischhauer, L., Chandhok, G., Guttmann, S., Avsar, Y., Guo, S., Ackermann, E. J., Gollob, J. et al. (2016). Evaluation of therapeutic oligonucleotides for familial amyloid polyneuropathy in patient-derived hepatocyte-like cells. *PLoS ONE* **11**, e0161455.
Nillegoda, N. B., Kirstein, J., Szlachcic, A., Berynskyy, M., Stank, A., Stengel, F., Arnsburg, K., Gao, X., Scior, A., Aebersold, R. et al. (2015). Crucial HSP70 co-chaperone complex unlocks metazoan protein disaggregation. *Nature* **524**, 247-251.
Norgren, N., Olsson, M., Nyström, H., Ericzon, B. G., de Tayrac, M., Genin, E., Planté-Bordeneuve, V. and Suhr, O. B. (2014). Gene expression profile in hereditary transthyretin amyloidosis: differences in targeted and source organs. *Amyloid* **21**, 113-119.
Ojha, J., Masilamoni, G., Dunlap, D., Udoff, R. A. and Cashikar, A. G. (2011). Sequestration of toxic oligomers by HspB1 as a cytoprotective mechanism. *Mol. Cell. Biol.* **31**, 3146-3157.
Ortmann, D. and Vallier, L. (2017). Variability of human pluripotent stem cell lines. *Curr. Opin. Genet. Dev.* **46**, 179-185.
Park, S. K., Arslan, F., Kanneganti, V., Barmada, S. J., Purushothaman, P., Verma, S. C. and Liebman, S. W. (2018). Overexpression of a conserved HSP40 chaperone reduces toxicity of several neurodegenerative disease proteins. *Prion* **12**, 16-22.
Patrosso, M. C., Salvi, F., De Grandis, D., Vezzoni, P., Jacobson, D. R. and Ferlini, A. (1998). Novel transthyretin missense mutation (Thr34) in an Italian family with hereditary amyloidosis. *Am. J. Med. Genet.* **77**, 135-138.
Radlovic, N., Lekovic, Z., Radlovic, V., Simic, D., Topic, A., Ristic, D., Ducic, S. and Baletic, A. (2014). Alpha-1-antitrypsin deficiency in children: clinical characteristics and diagnosis. *Srp. Arh. Celok. Lek.* **142**, 547-550.
Raju M., S., V, J., Kamaraju, R. S., Sritharan, V., Rajkumar, K., Natarajan, S., Kumar, A. D. and Burgula, S. (2016). Continuous evaluation of changes in the serum proteome from early to late stages of sepsis caused by Klebsiella pneumoniae. *Mol. Med. Rep.* **13**, 4835-4844.
Sakai, K., Asakawa, M., Takahashi, R., Ishida, C., Nakamura, R., Hamaguchi, T., Ono, K., Iwasa, K. and Yamada, M. (2017). Coexistence of transthyretin- and Abeta-type cerebral amyloid angiopathy in a patient with hereditary transthyretin V30M amyloidosis. *J. Neurol. Sci.* **381**, 144-146.
Santos, S. D., Magalhães, J. and Saraiva, M. J. (2008). Activation of the heat shock response in familial amyloidotic polyneuropathy. *J. Neuropathol. Exp. Neurol.* **67**, 449-455.
Sato, T., Susuki, S., Suico, M. A., Miyata, M., Ando, Y., Mizuguchi, M., Takeuchi, M., Dobashi, M., Shuto, T. and Kai, H. (2007). Endoplasmic reticulum quality control regulates the fate of transthyretin variants in the cell. *EMBO J.* **26**, 2501-2512.
Sato, T., Sako, Y., Sho, M., Momohara, M., Suico, M. A., Shuto, T., Nishitoh, H., Okiyoneda, T., Kokame, K., Kaneko, M. et al. (2012). STT3B-Dependent posttranslational N-glycosylation as a surveillance system for secretory protein. *Mol. Cell* **47**, 99-110.
Schreiber, G. (2002). The evolution of transthyretin synthesis in the choroid plexus. *Clin. Chem. Lab. Med.* **40**, 1200-1210.
Sekijima, Y., Hammarström, P., Matsumura, M., Shimizu, Y., Iwata, M., Tokuda, T., Ikeda, S. and Kelly, J. W. (2003). Energetic characteristics of the new transthyretin variant A25T may explain its atypical central nervous system pathology. *Lab. Invest.* **83**, 409-417.
Sekijima, Y., Wiseman, R. L., Matteson, J., Hammarström, P., Miller, S. R., Sawkar, A. R., Balch, W. E. and Kelly, J. W. (2005). The biological and chemical basis for tissue-selective amyloid disease. *Cell* **121**, 73-85.
Shoulders, M. D., Ryno, L. M., Genereux, J. C., Moresco, J. J., Tu, P. G., Wu, C., Yates, J. R., III, Su, A. I., Kelly, J. W. and Wiseman, R. L. (2013). Stress-independent activation of XBP1s and/or ATF6 reveals three functionally diverse ER proteostasis environments. *Cell Rep.* **3**, 1279-1292.
Suenaga, G., Ikeda, T., Masuda, T., Motokawa, H., Yamashita, T., Takamatsu, K., Misumi, Y., Ueda, M., Matsui, H., Senju, S. et al. (2017). Inflammatory state exists in familial amyloid polyneuropathy that may be triggered by mutated transthyretin. *Sci. Rep.* **7**, 1579.
Tang, H., Fu, Y., Zhan, S. and Luo, Y. (2009a). αEC, the C-terminal extension of fibrinogen, Has chaperone-like activity. *Biochemistry* **48**, 3967-3976.
Tang, H., Fu, Y., Cui, Y., He, Y., Zeng, X., Ploplis, V. A., Castellino, F. J. and Luo, Y. (2009b). Fibrinogen has chaperone-like activity. *Biochem. Biophys. Res. Commun.* **378**, 662-667.
Topic, A., Ljujic, M. and Radojkovic, D. (2012). Alpha-1-antitrypsin in pathogenesis of hepatocellular carcinoma. *Hepatitis Monthly* **12**, e7042.
van Oosten-Hawle, P. and Morimoto, R. I. (2014). Organismal proteostasis: role of cell-nonautonomous regulation and transcellular chaperone signaling. *Genes Dev.* **28**, 1533-1543.

Verma, M., Girdhar, A., Patel, B., Ganguly, N. K., Kukreti, R. and Taneja, V. (2018). Q-rich yeast prion [PSI(+)] accelerates aggregation of transthyretin, a non-Q-rich human protein. *Frontier. Mol. Neurosci.* **11**, 75.

Wang, X., Cattaneo, F., Ryno, L., Hulleman, J., Reixach, N. and Buxbaum, J. N. (2014). The systemic amyloid precursor transthyretin (TTR) behaves as a neuronal stress protein regulated by HSF1 in SH-SY5Y human neuroblastoma cells and APP23 Alzheimer's disease model mice. *J. Neurosci.* **34**, 7253-7265.

Wei, S., Episkopou, V., Piantedosi, R., Maeda, S., Shimada, K., Gottesman, M. E. and Blaner, W. S. (1995). Studies on the metabolism of retinol and retinol-binding protein in transthyretin-deficient mice produced by homologous recombination. *J. Biol. Chem.* **270**, 866-870.

Willander, H., Askarieh, G., Landreh, M., Westermark, P., Nordling, K., Keranen, H., Hermansson, E., Hamvas, A., Nogee, L. M., Bergman, T. et al. (2012a). High-resolution structure of a BRICHOS domain and its implications for anti-amyloid chaperone activity on lung surfactant protein C. *Proc. Natl. Acad. Sci. USA* **109**, 2325-2329.

Willander, H., Presto, J., Askarieh, G., Biverstål, H., Frohm, B., Knight, S. D., Johansson, J. and Linse, S. (2012b). BRICHOS domains efficiently delay fibrillation of amyloid beta-peptide. *J. Biol. Chem.* **287**, 31608-31617.

Wyatt, A. R., Yerbury, J. J., Dabbs, R. A. and Wilson, M. R. (2012). Roles of extracellular chaperones in amyloidosis. *J. Mol. Biol.* **421**, 499-516.

Yazaki, M., Yoshinaga, T., Sekijima, Y., Kametani, F. and Okumura, N. (2018). Hereditary fibrinogen Aalpha-chain amyloidosis in Asia: clinical and molecular characteristics. *Int. J. Mol. Sci.* **19**, 320.

Yerbury, J. J., Kumita, J. R., Meehan, S., Dobson, C. M. and Wilson, M. R. (2009). α2-Macroglobulin and haptoglobin suppress amyloid formation by interacting with prefibrillar protein species. *J. Biol. Chem.* **284**, 4246-4254.

Zsila, F. (2010). Inhibition of heat- and chemical-induced aggregation of various proteins reveals chaperone-like activity of the acute-phase component and serine protease inhibitor human α1-antitrypsin. *Biochem. Biophys. Res. Commun.* **393**, 242-247.